EPJ Web of Conferences **38**, 17001 (2012)
DOI: 10.1051/epjconf/20123817001

Investigation of the influence of incomplete fusion on complete fusion of ^{16}O induced reactions at moderate excitation energies

Avinash Agarwal[1,a], Sunil Dutt[1], Anjali Sharma[1], I.A. Rizvi[2], Kamal Kumar[2], Sabir Ali[2], Tauseef Ahamad[3], Rakesh Kumar[4], and A.K. Chaubey[5]

[1] Department of Physics, Bareilly College, Bareilly 243 005, India
[2] Department of Physics, Aligarh Muslim University, Aligarh, 202 002, India
[3] Girls Senior Secondary School, Aligarh Muslim University, Aligarh, 202 002, India
[4] Nuclear Physics Group, Inter University Accelerator Centre, New Delhi 110 067, India
[5] Depatment of Physics, Addis Ababa University P.O.Box 1176, Addis Ababa, Ethiopia

Abstract. An attempt has been made to investigate for the reaction dynamics leading to incomplete fusion (ICF) of heavy ions at moderate excitation energies, especially the influence of incomplete fusion on complete fusion (CF) of ^{16}O induced reactions at specific energies. Excitation functions (EFs) of various reaction products populated via CF and/or ICF of ^{16}O projectile with ^{45}Sc target were measured at energies ≈3-7 MeV/nucleon, using recoil catcher technique followed by offline γ-ray spectroscopy.The measured EFs were compared with theoretical values obtained using the statistical model code PACE4. The experimentally measured EFs were in general found to be in good agreement with the theoretical predictions for non α- emitting channels in the present target projectile system. However, for α-emitting channels the measured EFs were higher than the predictions of the theoretical model codes, which may be credited to incomplete fusion reactions at these energies.

1 Introduction

In recent years extensive efforts have been made to study the incomplete fusion (ICF) reaction dynamics, at energies in the vicinity of Coulomb barrier (CB). It has been a topic of extensive discussion among experimental as well as theoretical nuclear physicists in the past several years [1–6]. This discussion has been continuously innovated with the onset of competition between ICF and complete fusion (CF) reactions just above the CB [2,4]. Moreover, at relatively higher projectile energies the concept of critical angular momentum distinguishes both the reaction dynamics. As per sharp cut-off approximation, the probability of CF is assumed to be unity for $l \leq l_{crit}$ and zero in case of $l \geq l_{crit}$ [7]. Hence, at relatively higher projectile energies and at larger impact parameters, CF moderately gives way to ICF, where fractional mass and charge as well as the linear momentum of projectile are transferred to the target nucleus, due to the prompt emission of α-clusters in the forward cone with almost projectile energy. The studies of coincidence relationships between the outgoing α-particles and the discrete γ-rays of the heavy residues unambiguously has also proved that in these reactions a massive part of the projectile fuses with the target while that remaining escapes at forward angles carrying a large part of the kinetic energy and angular momentum [8]. Furthermore, a few reports [9–11] have shown that the population of low-spin states are observed to be hindered and/or less fed in the case of ICF. This reveals the occurrence of ICF due to the influence of centrifugal potential in the peripheral interactions, where driving angular momentum limits do not allow CF. Recently, CF reaction has been used to synthesize superheavy elements [12–15]. However, at these low energies, the evidence of ICF [1–4] along with fission and quasifission may be a cause of hindrance to achieve superheavy elements. These reactions were first observed by Britt and Quinton [16] with the experimental evidence of forward peaked α-particles in the interaction of heavy projectile target systems at energies ≈10.5 MeV/A. Particle-gamma coincidence studies by Inamura et al. [9] contributed strongly to the understanding of the mechanism of ICF reactions. Furthermore such reactions are difficult to explain in terms of deep inelastic collisions as the mass flow is always from projectile to target. Several theoretical models like Exciton model [17], Breakup fusion (BUF) model [18], Promptly emitted particles (PEPs) model [19], Multistep direct reaction theory [20] and Hot spot model [21] etc. have been proposed to explain ICF reaction dynamics. All these models were used to explain experimental data at energies ≈10 MeV/A. Some recent studies, however, showed the onset of ICF just above the Coulomb barrier. Parker et al. [22] observed forward peaked alpha-particles in reaction of low-Z heavy ions with energy 6 MeV/A on ^{51}V. Morgenstern et al. [23] observed ICF component in the velocity spectra of evaporation residues (ERs) in a reaction of ^{40}Ar with boron and carbon target. Tserruya et al. [24] found evidences for incomplete fusion from Time of Flight (TOF) measurements of ERs in a reaction at 5.5-10 MeV/nucleon energies of ^{12}C with ^{120}Sn, ^{160}Gd and ^{197}Au. Ismail et al. [25] measured excitation functions (EFs) and mean projectile recoil ranges of nuclei produced in the HI reactions using thick target – thick recoil catcher technique to study incomplete fusion reactions. M. Cavinato et al. [26] measured excitation functions, recoil range distribution and angular distribution

[a] e-mail: avibcb@gmail.com

Table 1. List of identified Evaporation Residues (ERs) and their spectroscopic data used in the present study

Reaction	half-life ($T_{1/2}$	Spin-parity (J^p)	E_γ KeV	I^γ %
^{57}Ni (p3n)	36.0 d	$3/2^-$	1376.8	77.6
^{56}Ni (p4n)	6.07 d	0^+	158.7	98.8
			480.0	36.5
^{57}Co(2p2n)	271.79 d	$7/2^-$	121.2	85.5
^{56}Co (αn)	78.76 d	4^+	846.6	100.0
			1036.9	14.0
			1237.6	67.6
^{55}Co (α2n)	17.56 h	$7/2^-$	477.2	20.3
			932.2	75.0
			1407.4	16.5
^{52}Fe (α4pn)	8.27 h	0^+	168.7	99.2
^{54}Mn (α2pn)	312.2 d	3^+	834.2	100.0
^{52g}Mn (2αn)	5.60 d	6^+	743.8	90.0
			934.9	94.5
			1433.5	100.0
^{51}Cr (2αpn)	27.7 d	$7/2^-$	319.7	10.0
^{48}V (3αn)	15.97 d	4^+	983.2	100.0

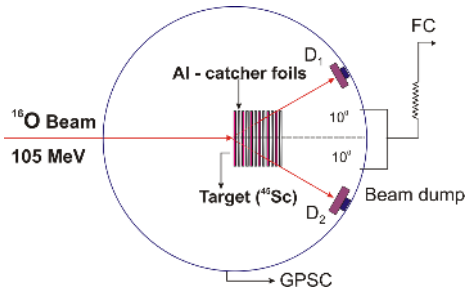

Fig. 1. Typical stacked foil arrangement used for excitation function measurement by activation technique.

of a great number of radioactive residues, providing evidences for the emission of preequilibrium nucleons during the thermalization of the composite nucleus and reproduce the excitation functions calculated within the Boltzmann master equation theory. B.S. Tomer et al. [27] explained ICF reactions in the framework of break-up fusion model and showed the entrance channel mass asymmetry dependence of ICF reactions in different exit channel. Recently, few groups in India [1–4, 28, 29] in their experiments tried to confirm the predictions of break-up fusion model of the incomplete fusion reactions by measurements of EFs and Forward Recoil Range Distributions (FRRD). Apart from that Dracoulis et al. [30], Lane et al. [31], and Mullins et al. [32] reported that ICF can selectively populate high spin states in final reaction products even at low bombarding energies and therefore can be used as a spectroscopic tool. More recently P. P. Singh [4, 11] observed large influence of incomplete fusion in his studies by measurement of spin distributions of evaporation residues at energy 5.6 MeV/A. However, a perfect modeling of ICF processes is still missing.

2 Experimental Details

The experiment was carried out using the general purpose scattering chamber (GPSC) facility found at the Inter University Accelerator Center (IUAC), New Delhi, India. A stack containing ^{45}Sc targets was irradiated by a ^{16}O beam at 105 MeV in the GPSC (the chamber has a facility of in-vacuum transfer of targets, which minimizes the time-lapse between the stopping of irradiation and the beginning of counting). A typical stacked foil arrangement used for excitation function measurements is shown in figure 1. The irradiation of the stack covered the desired energy range of ≈50-105 MeV in measuring the EFs of various evaporation residues produced in the ^{16}O + ^{45}Sc system. The beam current was ≈20 nA throughout the irradiation. The ^{45}Sc targets of thickness 1.42 mg/cm^2, backed by Al catchers of thickness 2 mg/cm^2, were placed after each target normal to the beam direction so that the recoiling nuclei coming out of the target could be trapped in the catcher foil and there would be no loss of activity. To ensure more efficient collection of CF and ICF products, the thickness of Al backings was carefully chosen. The incident flux of the ^{16}O beam was determined from the charge collected in the Faraday cup (using an ORTEC current integrator device), as well as from the counts of the two Rutherford monitors kept at ±10° to the beam direction. The two sets of values were found to agree with each other, any difference between them being within the 5% range (of the values). The stack was irradiated for ≈9 h, keeping in mind the half-lives of interest. The activities induced in the catcher-target assembly were followed off-line, using precalibrated CANBERAs HPGe detector coupled to CAMAC and based on the FREEDOM data acquisition system developed by the IUAC [33]. The average time between the end of the irradiation and the beginning of the measurements with HPGe was ≈15 min. The nuclear spectroscopic data used in the evaluation and measurement of cross sections were taken from the radioactive isotopes data table by Browne and Firestone [34] and are given in Table 1. The spectrometer was calibrated for energy, and efficiency was measured using various standard sources, i.e. ^{152}Eu, ^{57,60}Co, and ^{133}Ba. Details of geometry-dependent efficiency measurements used in this work are similar to those used by Ahamad et al. [28]. The residues produced from various reaction channels were identified by their characteristic γ-ray and decay curve analysis. The details of the experimental arrangements, formulations, and data reduction procedures used in the present work are similar to those in the

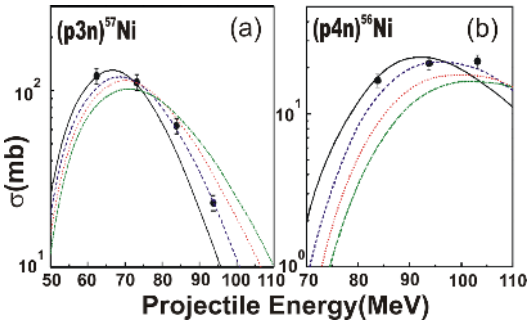

Fig. 2. Experimentally measured and theoretically calculated EFs for different residues populated via (p3n) and (p4n) channels in the ^{16}O + ^{45}Sc system at ≈50-105 MeV. The curves represent the theoretical predictions of the PACE4 statistical model code at different values of K: K = 8 (black solid line), 10 (blue dashed line), 12 (red dotted line) and 14(green dash-dotted line). The solid circles represent the measured cross-sections with associated errors.

work of Agarwal et al. [29]. The standard formulation reported in Ref. [35] was used to determine the production cross sections of various reaction products. The various factors that may introduce errors and uncertainties in the present cross-section measurements and their estimates are the following: (i) The non-uniform thickness of samples may lead to uncertainty in determining the number of target nuclei. To check the extent of the non-uniformity of the sample, the thickness of each sample was measured at different positions using α- transmission method. It is estimated that the error in the thickness of the sample materials is less than 1%. (ii) Fluctuation in the beam current may result in variation of the incident flux; proper care was taken to keep the beam current constant as much as possible. The error due to this factor was incorporated by taking the weighted average of the beam current and is estimated to be less than 2%. (iii) The dead time in the spectrometer may lead to a loss in the counts. By suitably adjusting the sample-detector distance, the dead time was kept below 10%. These errors exclude uncertainty of the nuclear data, such as branching ratio, decay constant, etc., which have been taken from Ref. [33]. (iv) Uncertainty in determining the geometry-dependent detector efficiency may also introduce some error, which is estimated to be less than 2%. (v) Errors due to a decrease in the oxygen ion beam intensity caused by scattering while transferring through the stack are estimated to be less than 1%. Attempts were made to minimize the uncertainties caused by all the above factors. The overall error in the present work is estimated to be less than or equal to 17%.

3 Experimental results and analysis

EFs for residues produced in the ^{16}O + ^{45}Sc system via CF and/or ICF processes were measured at projectile energies up to 105 MeV. To investigate the ICF reaction dynamics, the EFs for ^{57}Ni, ^{56}Ni, ^{57}Co, ^{56}Co, ^{55}Co, ^{52}Fe, ^{54}Mn, ^{52}Mn, ^{51}Cr, and ^{48}V radionuclides produced in this energy range were considered. The cross sections from a given reaction channel were determined separately from the observed intensities of all possible identified γ-rays, arising from the same radionuclide. The reported values are the weighted average of the various cross-section values obtained [35]. An analysis of experimentally measured EFs was made by comparing them with the theoretical predictions of the statistical model code, PACE4 [36]. The PACE4 code uses a Monte Carlo procedure to determine the decay sequence of an excited nucleus using the Hauser- Feshback formalism. This formalism takes angular momentum directly into account. The angular momentum projections are calculated at each stage deexcitation, which enables the determination of the angular distribution of emitted particles.

The other details of model calculations can be found in our earlier publications [1,29]. The measured EFs along with theoretical predictions obtained using the PACE4 code for representative residues populated via non α - emitting channels, (p3n) and (p4n) are shown in figure 2. In these sets of channels, there is no likelihood of ICF reactions, and therefore, this set of channels are populated only by CF. As can be seen from figure 2 the calculated EFs corresponding to the level density parameter K=10 in general reproduced satisfactorily experimentally measured EFs for the residues ^{57}Ni and ^{56}Ni produced in the CF reactions

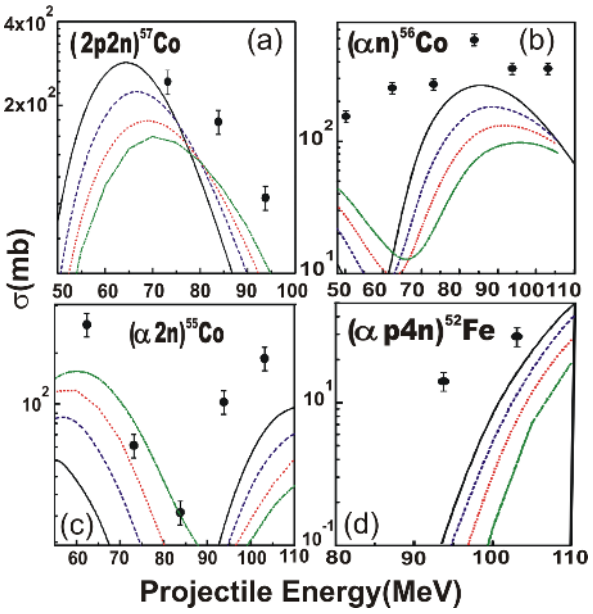

Fig. 3. Experimentally measured and theoretically calculated EFs for different residues populated via (2p2n), (α,n),(α,2n) and (α,p4n) channels in the ^{16}O + ^{45}Sc system at ≈50-105 MeV. The other details are same as in figure 2.

of the ^{16}O projectile with the ^{45}Sc target, which is consistent with our earlier findings [1]. The EFs for the reaction channel (2p2n) is shown in figure 3(a). An agreement between theoretical and experimental values exists at 73.2 ± 2.8 MeV and above this energy significant enhancement of cross-section is found. This simply indicates that ^{57}Co is populated via CF and ICF of ^{8}Be fragment both. Regarding the residues ^{56}Co, ^{55}Co , ^{52}Fe and ^{54}Mn, populated through (α,n), (α,2n), (α,p4n), and (α,2pn) channels, it is obvious from figures 3(b - d) and figure 4(a) that our measured cross-sections are higher than the theoretical predictions. This enhancement can be explained by the ICF of ^{12}C fragment of the projectile to the target. Figures 4(b) and 5 show the EFs for the residues ^{52}Mn, ^{51}Cr and ^{48}V populated by the channels (2α,n) (2α,pn) and (3α,n). It can be seen from the figures that measured excitation functions are much higher but in the same trend as the theoretically calculated values, which can be explained by assuming that these channels are populated not only by CF but also with ICF of ^{8}Be fragment (in case of ^{52}Mn and ^{51}Cr) and ^{12}C fragment (in case of ^{48}V) of projectile to the target.

4 Conclusions

The excitation functions for the (O,p3n), (O,p4n), (O,2p2n), (O,αn), (O,α2n), (O,αp4n), (O,α2pn), (O,2αn), (O,2αpn) and (O,3αn) reactions for ^{16}O + ^{45}Sc system have been measured in the energy range 50-105 MeV. The comparative study of experimentally measured excitation functions with theoretical predictions show the considerable enhancement in cross-sections for ^{57}Co, ^{56}Co, ^{55}Co, ^{52}Fe, ^{54}Mn, ^{52}Mn, ^{51}Cr and ^{48}V nuclides indicating that the processes other than compound nucleus formation are playing an important role in the production of these isotopes. The large difference in our measured and calculated values gives clear signatures of incomplete fusion for these

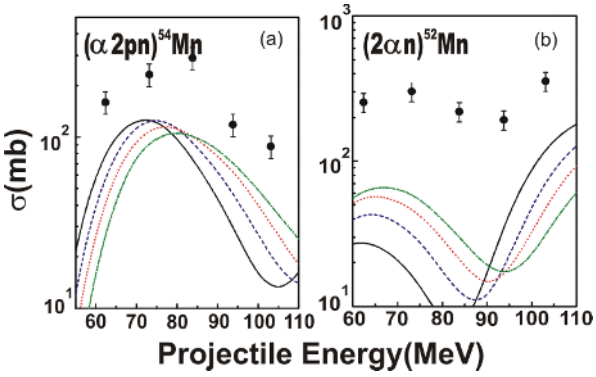

Fig. 4. Experimentally measured and theoretically calculated EFs for different residues populated via (α,2pn) and (2α,n) channels in the ^{16}O + ^{45}Sc system at ≈ 50-105 MeV. The other details are same as in figure 2.

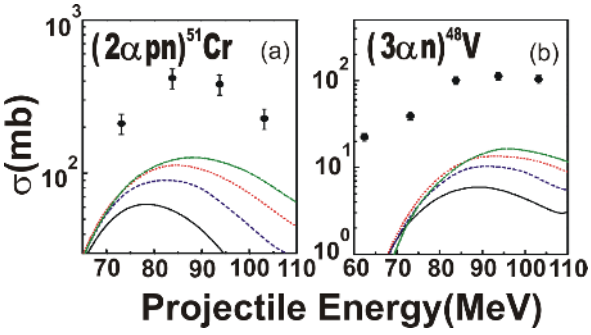

Fig. 5. Experimentally measured and theoretically calculated EFs for different residues populated via (2α,pn) and (3α,n) channels in the ^{16}O + ^{45}Sc system at ≈50-105 MeV. The other details are same as in figure 2.

channels in the considered energy range. Moreover, for a perfect modeling of the ICF process, more detailed experiments consisting of the measurement of forward recoil range distributions and spin distribution of residues populated by CF as well ICF, using particle-gamma coincidence technique both at relatively low and higher bombarding energies are desirable.

Acknowlegements

The authors are thankful to the Director IUAC, New Delhi for providing all the necessary facilities to carry out the experiment. Thanks are also to **Dr. R. P. Singh**, Principal, Bareilly College, Bareilly for his keen interest in the present study. One of the author (SD) is thankful to UGC (India) for financial support through JRF in Major research Project **Ref. F. No. 40-430/2011 (SR)**. Financial support from DST (India) through Young Scientist Scheme **Ref. No. SR/FTP/PS-08/2006** to one of author (AA) is also highly acknowledged.

References

1. F.K. Amanuel, *et al.*, Phys. Rev. C **84**, 024614 (2011)
2. Abhishek Yadav, *et al.*, Phys. Rev. C **85**, 034614 (2012)
3. Devendra P. Singh, *et al.*, Phys. Rev. C **80**, 014601 (2009)
4. Pushpendra P. Singh, *et al.*, Phys. Rev. C **77**, 014607 (2008)
5. A. Diaz-Torres, *et al.*, Phys. Rev. Lett. **98**, 152701 (2007)
6. A. Diaz-Torres, *et al.*, Phys. Rev. C **65**, 024606 (2002)
7. J. Wilczynski, *et al.*, Phys. Rev. Lett. **45**, 606 (1980)
8. K. Surendra Babu, *et al.*, J. Phys. G: Nucl. Part. Phys. **29**, 1011(2003)
9. T. Inamura, *et al.*, Phys. Lett. B **68**, 51 (1977)
10. Pushpendra P. Singh, *et al.*, Phys. Lett. B **671**, 20 (2009)
11. Pushpendra P. Singh, *et al.*, Phys. Rev. C **80**, 064603 (2009)
12. K. Siwek Wilczynska *et al.*, Phys. Rev. C **72**, 034605 (2005)
13. V.I. Zagrebaev, Nucl. Phys. A **734**, 164 (2004)
14. Robert Smolanczuk, Phys. Rev. C **59**, 2634 (1999)
15. Sushil Kumar, *et al.*, J. Phys. G: Nucl. Part. Phys. **29**, 625 (2003)
16. H.C. Britt and A.R. Quinton, Phys. Rev. **124**, 877 (1961)
17. M. Blann, *et al.*, Phys. Rev. Lett. **27**, 337 (1971)
18. T. Udagawa and T. Tamura, Phys. Rev. Lett. **45**, 1311 (1980)
19. J.P. Bondrof, Nucl.Phys. A **333**, 285 (1980)
20. V.I. Zagrebaev, Ann. Phys. (NY) **197**, 33 (1990)
21. R. Weiner, *et al.*, Nucl. Phys. A **286**, 282 (1977)
22. D.J. Parker, *et al.*, Phys. Rev. C **39**, 2256 (1989)
23. H. Morgenstern, *et al.*, Phys. Rev. Lett. **52**, 1104 (1984)
24. I. Tserruya, *et al.*, Phys. Rev. Lett. **60**, 14 (1988)
25. M. Ismail, *et al.*, Pramana. J. Phys. **52**, 609 (1999)
26. M. Cavinato, *et al.*, Phys. Rev. C **52**, 2577 (1995)
27. B.S. Tomar, *et al.*, Phys. Rev. C **49**, 941 (1994)
28. T. Ahamad, *et al.*, Int. J. Mod. Phys. E **20** , 645 (2011)
29. Avinash Agarwal, *et al.*, Int. J. Mod. Phys. E **17**, 393 (2008)
30. G.D. Dracoulis, *et al.*, J. Phys. G: Nucl. Part. Phys. **23**, 1191 (1997)
31. G.J. Lane, *et al.*, Phys. Rev. C **60**, 067301 (1999)
32. S.M. Mullins *et. al.*, Phys. Lett B **393**, 279 (1997); Phys. Rev. C **61**, 044315 (2000)
33. FREEDOM, *Data acquisition and analysis software, designed to support accelerator based experiments at the IUAC, New Delhi, India.*
34. E. Browne and R.B. Firestone, V.S. Shirley, *Table of Radioactive Isotopes* (Wiley, New York, 1986)
35. S.F. Mughabghab, *et al.*, *Neutron Cross-Sections* (Academic Press, New York, 1981), Vol. 1, Part A, p. 89.
36. A. Gavron, Phys. Rev. C **21**, 230 (1980)